I Walk an Ancient Road: A Straightforward Methodology for Analyzing Intra- and Inter-regional Connectivity Systems along Roman Frontier Zones

Supplemental Materials

https://doi.org/10.25365/phaidra.540

Dominik Hagmann

Department of Evolutionary Anthropology
Human Evolution and Archaeological Science
University of Vienna
Djerassiplatz 1
1030 Vienna
Austria

https://orcid.org/0000-0002-4481-6234
dominik.hagmann@univie.ac.at

Version 1.0.0 | 2024-09-24

Table of contents

1 Introduction ... 2
2 Section 1: Site definition by applying Nearest Neighbour Analysis (NNA) and Density-based Spatial Clustering of Applications with Noise (DBSCAN) ... 3
2.1 Data sources ... 3
2.2 Software used ... 3
2.3 Description ... 3
2.4 Results ... 9
3 Section 2: Least cost analysis (LCA) ... 10
3.1 Data sources ... 10
3.2 Software used ... 10
3.3 Description ... 10
3.3.1 Least-cost Paths (LCPs) ... 10
3.3.2 Cost Surface 01: Least-cost Site Catchment Analysis (LCSCA) ... 10
3.3.3 Cost Surface 02: Hydrology and slope ... 11
3.3.4 Line density ... 12
3.4 Results ... 12
4 Section 3: Spatial social network analysis (SSNA) ... 13
4.1 Data source ... 13
4.2 Software used ... 13
4.3 Description ... 13
4.4 Results ... 13
5 Section 4: Visibility analysis (VA) ... 14
5.1 Data source ... 14
5.2 Software used ... 14
5.3 Description ... 14
5.4 Results ... 14
6 Section 5: Ground truthing ... 15
6.1 Data source ... 15
6.2 Hardware used ... 15
6.3 Software used ... 15
6.4 Description ... 15
7 References ... 17

1 Introduction

These supplemental materials serve as a comprehensive "user guide" for the paper "I Walk an Ancient Road: A Straightforward Methodology for Analyzing Intra- and Inter-regional Connectivity Systems along Roman Frontier Zones (c. 1st — 5th century AD)." The materials are designed to be easy to reproduce, readable, and understandable for all users. They are free to use, adapt, and further develop, with all relevant data sources and results linked where they are directly included as supplementary data. In cases where results are not provided here, they can be found in the corresponding paper.

2 Section 1: Site definition by applying Nearest Neighbour Analysis (NNA) and Density-based Spatial Clustering of Applications with Noise (DBSCAN)

2.1 Data sources

- Archaeological features: Hagmann (2024)

2.2 Software used

- QGIS 3.34.x-Prizren: https://www.qgis.org/
- Nearest neighbour analysis tool in QGIS: https://github.com/qgis/QGIS-Documentation/blob/master/docs/user_manual/processing_algs/qgis/vectoranalysis.rst#nearest-neighbour-analysis
- DBSCAN clustering tool in QGIS: https://github.com/qgis/QGIS-Documentation/blob/master/docs/user_manual/processing_algs/qgis/vectoranalysis.rst#dbscan-clustering
- Mean coordinate(s) tool in QGIS: https://github.com/qgis/QGIS-Documentation/blob/master/docs/user_manual/processing_algs/qgis/vectoranalysis.rst#mean-coordinates

2.3 Description

The dataset used is an excerpt from the official national find registry of the Austrian Monuments Authority ("Fundstellendatenbank des Bundesdenkmalamtes"), which has been fundamentally revised. It consists of 1,184 Roman-era features across 551 spatial locations. To facilitate further analysis, these features need to be consolidated into meaningful sites. A feature in this context can range from a single coin find to a more complex object like a pottery kiln or an elaborate structure such as a gate. The database employs a marginally standardized chronology scheme, mostly allowing dating into broader phases (e.g., "Late Antiquity" from 284 to 488 AD) (Hagmann, in press/2024). The detailed characteristics of the database have been published, and the data has been made available as open data in Hagmann (2024).
Due to the heterogeneous ontological structure of the dataset, a careful approach is required to establish optimal analysis conditions. This involves key considerations regarding the definition of a site.:Without addressing the broader site definition debate, a "site" in the present context is understood as "a grouping of finds and features within a specific area." The approach acknowledges the data's diversity and defines sites based on the spatial relationships between find locations. Clusters of a certain size are treated as part of the same site, even though these clusters lack clear boundaries. These groupings effectively identify related objects, forming what can be described as a "relative activity zone" consisting of various finds and features (Bintliff, 2000; Bintliff & Snodgrass, 1988; Forbes, 2013; Gallant, 1986; McCoy, 2020; Mehrer & Westcott, 2006; Pelgrom, 2018; Rivers et al., 2013; Witcher, 2012).
Following this site-definition hypothesis, initial testing involved a visual inspection of site distribution, followed by a Nearest Neighbor Analysis (NNA) to formally analyze spatial relationships and identify potential clusters. This approach helped to recognize the groupings of finds and features based on their proximity and distribution patterns (Ducke, 2015; Orton, 2004). Methods such as interpolation of additional points or Monte Carlo simulations were not employed in this analysis.
The NNA was conducted in QGIS to analyze site distribution, categorizing spatial patterns as clustered, random, or dispersed. Particular attention was given to the shape of the survey area and the ratio of surveyed points to the survey area, as the same point pattern may appear random in a smaller area but clustered in a larger one. In the QGIS tool used, the survey area is defined by the smallest possible area containing the points, and no additional area could be included in the calculation. In the course of the NNA, the distances in meters from each site to its nearest neighbor, which are then averaged as the "observed mean distance" (OMD). This is compared to the "expected mean distance" (EMD) of randomly distributed simulated points. A lower OMD than the EMD indicates clustering, while a higher

OMD suggests a uniform distribution. Independent random processes (IRPs) assess whether all locations have equal probability (first-order effect) or influence each other (second-order effect). First-order effects are based on variations in underlying properties, while second-order effects arise from interactions between events. A null hypothesis test compared the observed site distribution to a random pattern generated by an IRP, or complete spatial randomness (CSR), assuming a random distribution. The "nearest neighbor index" (NN_{Index}), calculated by dividing the OMD by the EMD, clearly indicates the spatial pattern (Formula 1).

$$NN_{Index} = OMD/EMD \qquad \text{Formula 1}$$

NN_{Index} = nearest neighbor index, OMD = observed mean distance, EMD = expected mean distance

An NN_{Index} value < 1 indicates a cluster formation, a value > 1 indicates a uniform distribution, a value = 1 indicates a random distribution. Finally, a very high or very low Z-score indicates in the context of the NNA whether the process underlying the classified distribution pattern can be considered random in the sense of the IRP or not; a negative Z-score issued by the tool indicates no random distribution, while a high one indicates a random distribution (Casarotto, 2017; Clark & Evans, 1954; Gimond, 2024; Pinder et al., 1979) (Table 1).

Table 1: Results of the NNA for the AOI for the site locations (n = 551)

Label	Value (meters)
Observed mean distance (OMD)	355, 04607393359
Expected mean distance (EMD)	990, 81703723262
Number of points	551
Nearest neighbor index (NNIndex)	0, 35833666620
Z-Score	-28, 81468694982

Based on the 551 site locations, a nearest neighbor index of 0.358 and a Z-score of -28.815 were determined, allowing the rejection of the null hypothesis of an IRP distribution. This indicates that site clusters are clearly present in the study area. These clusters represent zones with higher concentrations of finds and features compared to surrounding areas within the Area of Interest (AOI).

Given the presence of site clusters identified by the NNA, the next step was to archaeologically define and visualize these clusters in QGIS. Since the number of clusters was unknown, a standard Density-Based Spatial Clustering of Applications with Noise (DBSCAN) algorithm was selected. This algorithm, developed by Ester, Kriegel, Sander, and Xu in 1996, is suitable for identifying clusters without requiring a predetermined number of clusters. In QGIS, a 2D Euclidean implementation of DBSCAN was applied to the point data representing features. The DBSCAN algorithm relies on two parameters: the minimum number of points per cluster (minPts) and the maximum distance (Ɛ), which defines the radius of a "catchment" area around each point for cluster formation. Points that meet the minPts requirement within their own catchment are designated as core points, and those within Ɛ of each other are considered directly density-reachable, forming clusters. Core points are symmetrically connected, as they are mutually density-reachable within the Ɛ limit. However, the algorithm also identifies border points, which lie within the catchment of a core point but do not meet the minPts requirement themselves. These border points are asymmetrically related to core points because they are reachable only through the core points. Despite this asymmetry, both core and border points belong to the same cluster and are density-connected. Points located outside any catchment area are classified as noise and are excluded from clustering. The algorithm processes each point sequentially, depending on the dataset, first identifying core points by evaluating whether they meet the minPts requirement within the Ɛ distance. Noise points are then identified as those that do not belong to any cluster. Border points are assigned to clusters based on their proximity to core points. However, in cases where a border point could belong to multiple clusters, the DBSCAN algorithm assigns it to just one cluster based on the processing sequence, which introduces a non-deterministic element. Core and noise points, by contrast, are deterministically classified. In this study, furthermore a special case arose: since the dataset includes isolated sites that may represent significant structures or features, though this cannot be determined from the dataset alone, the minimum cluster size was set to

1 (minPts = 1), treating each point as a core point. As a result, no border points were identified, and every point that would have been classified as noise if minPts > 1 functioned as "de-facto core points" or "pseudo-noise," as these points were always stand-alone core points located outside larger clusters. Core points in clusters were always directly density-reachable and symmetrical, with the smallest clusters consisting of pairs of core points. However, DBSCAN effectively grouped sites within specified distances while also incorporating isolated sites into the analysis (Clark & Evans, 1954; Ducke, 2015; Ester et al., 1996; Orton, 2004; Schubert et al., 2017; Hagmann, in press/2024). (Figure 1)

Different distance values were tested to determine the most suitable maximum distance (ε) for clustering, with a social-archaeological interpretation guiding the selection. In the AOI, each ε value in meters corresponds to a circular area, calculated using Formula 2. This circular area represents the effective catchment for the DBSCAN algorithm. The choice of ε depends on the research question and the archaeological significance of the site clusters. The assumption is that each cluster of finds and features represents a military, civilian, or urban settlement, spatially distinct from others. The distance ε should be large enough to prevent excessive cluster formation, but not so small that it divides sites that were historically connected.

A key limitation of DBSCAN is the need to decide in advance the most appropriate ε, which may not apply uniformly across all sites. Since most sites lack detailed information on their exact nature, location, or connection to other sites, generalized parameters are used. Even with different ε values for each site, it remains difficult to determine which parameters best reflect historical reality. In rare cases, complete data (e.g., from geophysical surveys) is available, but this is uncommon, and even then, site definition questions may become moot, making clustering unnecessary. Furthermore, while it would be interesting to cluster sites based on chronological parameters, likely shifting them across periods, this falls outside the scope of the current study. Here, the focus is on a basic clustering attempt for all AOI sites using the DBSCAN algorithm. Despite these limitations, DBSCAN offers a method to describe the ancient settlement pattern by identifying clusters in the data, even if the results are an approximation. This analysis allows for a spatial interpretation of the Roman settlement landscape under controlled, repeatable conditions, providing a basis for further exploration.

Comparative archaeological examples from classical antiquity, such as those from survey literature (cf., e.g., Bintliff, 2012; Wilkinson, 1989), provide additional context. Although surface find patterns influenced by practices like fertilization are more common in the Mediterranean and may not directly apply to the AOI, this data still offers useful references for estimating settlement activity zones relevant to the area (Table 2). The point coordinates of the clusters were visualized in QGIS by calculating the center of mass for each cluster. These centers of mass serve purely for visualization, representing the approximate central point of each "site." Given the nature of the data and the understanding of a site as an accumulation of archaeological objects reflecting related human activities over a specific time span, the calculated center may not correspond to the actual social focal point or any significant activity area within the group of sites. Nonetheless, this method offers a consistent and transparent approach to defining sites (Verhagen et al., 2016, pp. 310–311).

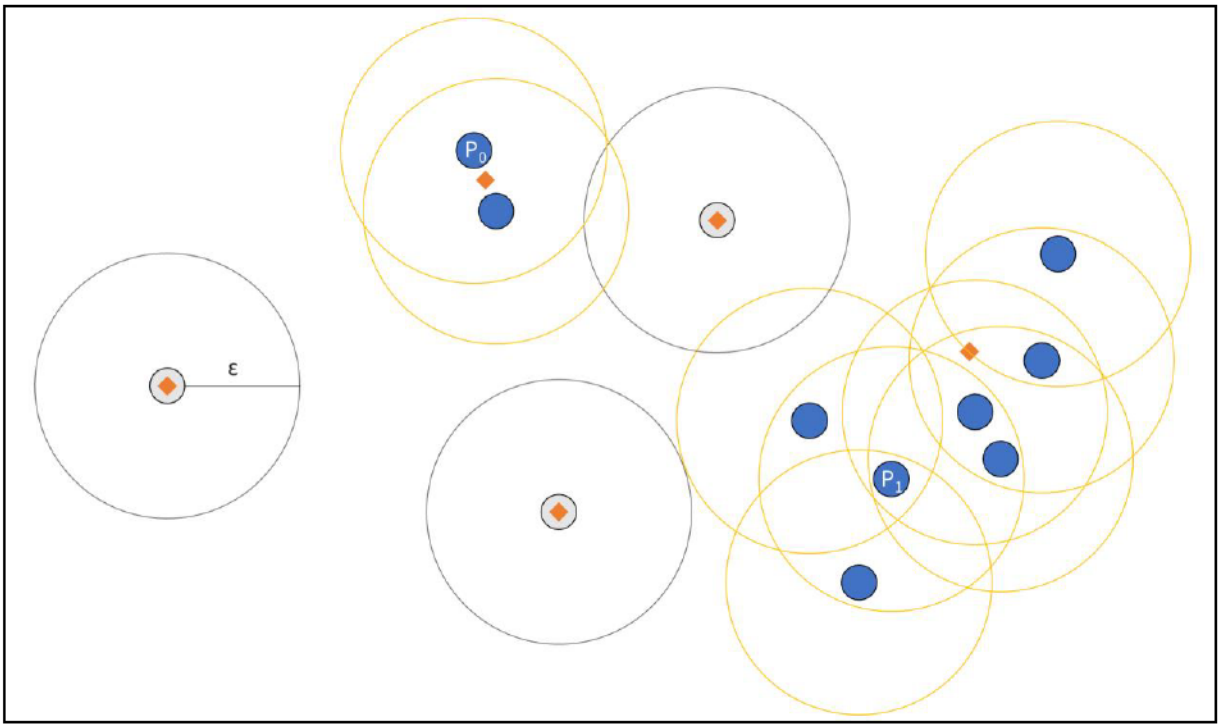

Figure 1: Illustration of the DBSCAN algorithm with minPts = 1 and maximum distance ε – Blue points (e.g., P0 and P1) with yellow catchment areas represent core points. All blue points are symmetrical and directly density-reachable, as they are within the maximum distance ε of each other, forming clusters. This also applies to pairs of core points forming two-point clusters. Since minPts = 1, all points are treated as core points, meaning there are no border points or traditional noise points. However, gray points behave similarly to noise ("pseudo-noise") as they are isolated from larger clusters. Orange diamonds indicate the center of mass of the clusters.

$$A = \pi \times r^2$$ **Formula 2**

A = area, r = ε.

Table 2: Extent of surface find scatter in relation to corresponding settlement types, according to Bintliff (2012, 113. 114 Fig. 4 A); Wilkinson (1989, 44 Tab. 1)

Settlement type	Settlement size	Radius of the surface find distribution (ε)	Area (m^2)
Hamlets and farmsteads	< 1.5 ha	200 - 400 m	13 - 50 ha
Villages	2 - 9 ha	600 - 1000 m	113 - 314 ha
Small towns	10 - 29 ha	1300 m	531 ha
Large cities	> 40 ha	2200 - 6000 m	15 km^2 - 113 km^2

A value of 355 m for ε, derived from the NNA's OMD and comparable to the find-dispersal considerations for hamlets and farmsteads (Table 2), corresponds to an area of approximately 40 ha and yielded 190 clusters. However, several findspots appeared in locations where a single larger findspot seemed more appropriate based on site definition criteria. Increasing ε to 450 m, corresponding to a catchment area of approximately 64 ha (positioned between larger farmsteads and smaller villages), resulted in 169 clusters. This value was chosen to test the effect of larger thresholds, as multiple clusters were still detected in areas where only one was expected. A radius ε = 1000 m, corresponding to the catchment of larger villages (approx. 314 ha), resulted in 103 clusters. However, this value seemed too high, as it grouped sites across clear topographical barriers like valleys and mountain slopes, creating overly large, spatially unclear clusters. An analysis with ε = 1480 m, representing the Roman measure of 1 MP (mille passus; Schulzki, 2006b) and a catchment of about 688 ha, further expanded the clustering. Based on the values in Table 2, a value of

740 m (0.5 MP), representing a catchment area of 172 ha, proved to be the most effective in the GIS-based comparison. Therefore using $\varepsilon = 740$ m and minPts = 1 in DBSCAN resulted in a well-distributed arrangement of 129 clusters, aligning with the topography and providing a logical summary of the sites. (Table 3; Figure 2)

Eventually, 129 mass focal points were determined and visualized, marking their abstract locations for distribution and overview maps. The results based on the 740 m maximum distance are well illustrated by the sites in the Traisen valley area, where clusters were formed that respect topographical features like hills and waterways. (Figure 3) This indicates that rural site clusters align with natural barriers, while more complex sites, such as the Auxiliary Fort of Augustianis/Traismauer on the right bank of the Traisen, are effectively grouped into clearly defined clusters. Scattered rural sites beyond the river are also sensibly clustered.

The chosen distance of 0.5 MP (740 m) accommodates all expected categories of rural settlements—hamlets, farmsteads, and smaller villages—as outlined in Table 2. The site clusters often display irregular shapes, with a halo-like thinning of finds from the central on-site area to the off-site periphery. The farther a site is from the mass focus (the abstract center), the fewer find spots occur. This pattern is also visualized with Voronoi diagrams: smaller polygons form in central areas of complex sites, while larger polygons reflect more dispersed peripheral sites. Combining Voronoi diagrams with site centers produces irregular shapes—round, arched, elongated, or polygonal—likely representing the on- and off-site areas and their surrounding halos.

The DBSCAN-based approach used here provides an approximation of the settlement's spatial distribution. However, the clustering also highlights limitations, as some sites are added to clusters based on their processing sequence, despite being spatially closer to other clusters. Interestingly, the most promising clustering results aligns with the Roman measure of 0.5 MP (740 m), suggesting the influence of Roman units of measurement, particularly the Roman mile, rather than other systems such as leugae (Schulzki, 2006a).

Table 3: DBASCAN-based clustering of the Roman sites in the AOI: parameters used

ε	Surface area	Catchment	Number of clusters (minPts = 1)
355 m	395919 m2	40 ha	190
450 m	636172 m2	64 ha	169
740 m	1720336 m2	172 ha	129
1000 m	3141592 m^2	314 ha	103
1480 m	6881344 m2	688 ha	64

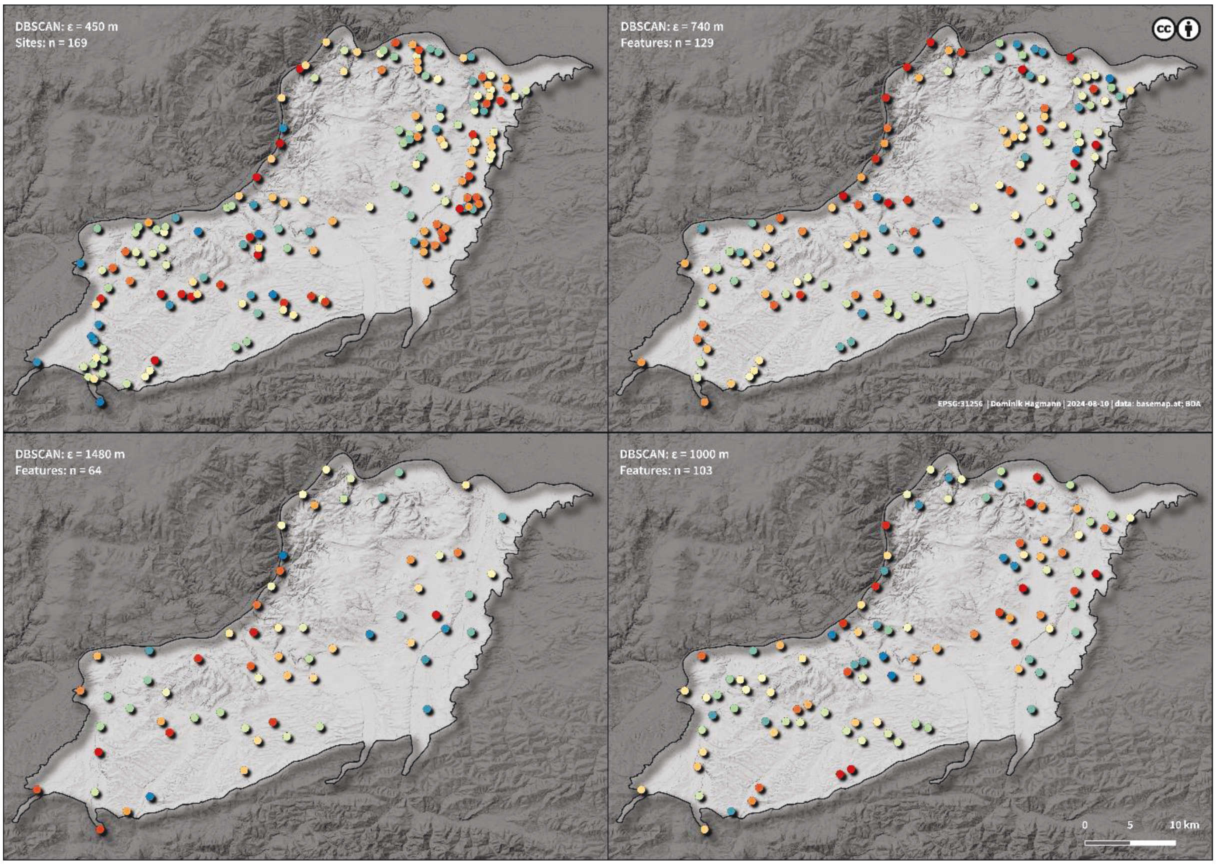

Figure 2: Visualization of the mass centroids of different DBSCAN clusters (clockwise, starting at the bottom left): Each panel represents a different maximum distance ε (450 m, 740 m, 1000 m, 1480 m) used for clustering, with minPts set to 1 in all cases. Compare Table 3 for the corresponding number of site clusters (data: Hagmann, 2024; Province of Lower Austria; basemap.at).

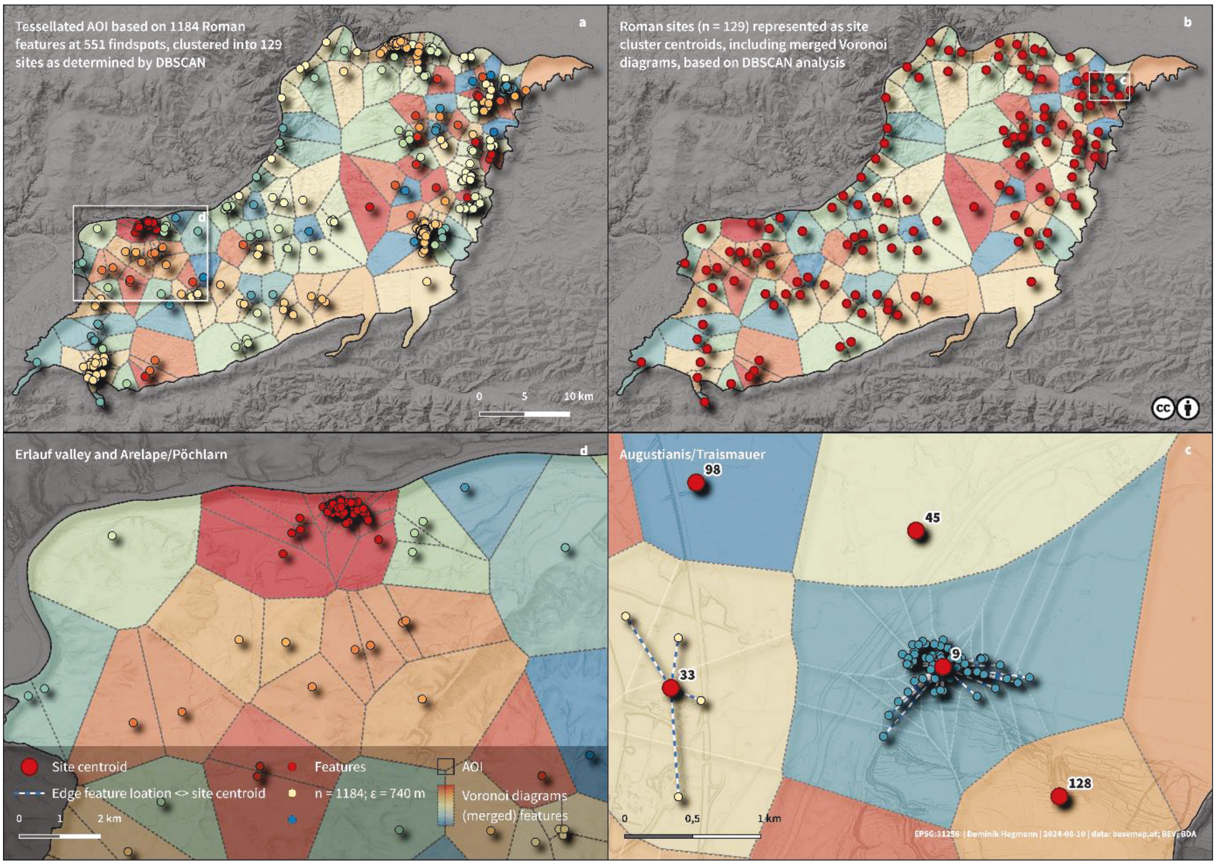

Figure 3 Illustration of the results of site clustering using DBSCAN (ε = 740 m; minPts = 1; top right and bottom right) compared to the data basis consisting of 1184 archaeological features (top left and bottom left). The data basis shows a dispersed landscape of isolated findspots, such as those around the location of the castellum Arelape/Pöchlarn and its hinterland. In contrast, the DBSCAN clustering clearly highlights a significant cluster of numerous sites near the castellum Augustianis (Traismauer; bottom right) and the grouping of scattered sites west of the Traisen River. The center of mass of each site is marked by a red dot, while the lines indicate the distance between the abstract site center and the actual findspots. The background Voronoi diagrams, with the sites as centers, demonstrate that point density increases towards the center of the area (data: Hagmann, 2024; Province of Lower Austria; basemap.at).

2.4 Results

- I Walk an Ancient Road: A Straightforward Methodology for Analyzing Intra- and Inter-regional Connectivity Systems along Roman Frontier Zones. Open Supplementary Data: https://doi.org/10.25365/phaidra.536

3 Section 2: Least cost analysis (LCA)

3.1 Data sources

- I Walk an Ancient Road: A Straightforward Methodology for Analyzing Intra- and Inter-regional Connectivity Systems along Roman Frontier Zones. Open Supplementary Data: https://doi.org/10.25365/phaidra.536
- Digital Terrain Model (10 x 10 m): https://www.data.gv.at/katalog/de/dataset/land-noe-digitales-hohenmodel-10-m
- Watercourses: https://doi.org/10.48677/c549b707-c9a2-459f-819e-2021a475a25e
- Floodplains (average recurrence interval of 300 years): https://www.data.gv.at/katalog/de/dataset/hochwasserabflussbereiche-hw300etc

3.2 Software used

- QGIS 3.34.x-Prizren: https://www.qgis.org/
- ArcGIS Pro 2.6.x: https://www.esri.com/en-us/arcgis/products/arcgis-pro/overview
- Slope tool in QGIS: https://github.com/qgis/QGIS-Documentation/blob/master/docs/user_manual/processing_algs/gdal/rasteranalysis.rst#slope
- Buffer tool in QGIS: https://github.com/qgis/QGIS-Documentation/blob/master/docs/user_manual/processing_algs/qgis/vectorgeometry.rst#buffer
- Least Cost Path plugin in QGIS: https://github.com/Gooong/LeastCostPath
- Line Density tool in QGIS: https://github.com/qgis/QGIS-Documentation/blob/master/docs/user_manual/processing_algs/qgis/interpolation.rst#line-density
- Mosaic To New Raster (Data Management) in ArcGIS Pro: https://pro.arcgis.com/en/pro-app/2.6/tool-reference/data-management/mosaic-to-new-raster.htm
- Path Distance tool in ArcGIS Pro: https://pro.arcgis.com/en/pro-app/latest/tool-reference/spatial-analyst/path-distance.htm

3.3 Description

3.3.1 Least-cost Paths (LCPs)

For the calculation of isotropic LCPs the “Least Cost Path” plugin in QGIS was used. The route-finding algorithm used is the Dijkstra algorithm, developed by Dutch computer scientist E. Dijkstra in 1959. This "greedy" algorithm seeks to consistently determine the most cost-effective path between an origin point and a target location on a surface (Dijkstra, 1959; Surface-Evans & White, 2012, p. 4).

3.3.2 Cost Surface 01: Least-cost Site Catchment Analysis (LCSCA)

Cost Surface 01, rooted in the concept of Site Catchment Analysis (SCA), is closely connected to Least Cost Site Catchment Analyses (LCSCAs), which refine traditional SCA by incorporating least-cost path models to more accurately assess the accessibility and resource-gathering potential of areas surrounding a site. SCA was first formally introduced by C. Vita-Finzi and E. Higgs in 1970 and examines the relationship between a site and its surrounding landscape, using GIS-based methods and without relying on direct archaeological fieldwork. A site catchment, or catchment area, refers to the "region accessible from a site," and is often analyzed in archaeological studies to evaluate the resources available in that area. SCA remains a "classic method" for understanding how inhabitants of archaeological sites engaged with their environment. Its primary aim is to define the area used for resource gathering, thereby assessing the mobility and economic potential available to ancient populations. As shown in Formula 3, Tobler's hiking function (1993) was used to calculate site catchments in the context of an LCSCA, serving as the cost function for the slope map to assess the travel time costs needed to traverse distances within the

AOI (Bailey, 2005, pp. 172–173; Becker et al., 2017, p. 1; Conolly & Lake, 2006, p. 214; Herzog, 2014, p. 232, 2020, p. 333; Legg, 2008; Vita-Finzi et al., 1970; Wheatley & Gillings, 2002, pp. 159–163).

$$W = 6^{-3,5 * abs(S+0,05)}$$ **Formula 3**

W **= walking velocity in km/h,** ***S*** **= slope as the mathematical gradient of a line (slope gradient in % / 100).**

For LCSCA, the "Path Distance" tool in ArcGIS Pro was used. As outlined in Formula 3, the walking velocity is calculated in km/h based on the slope, which is defined as the mathematical gradient of a line (slope gradient in % divided by 100). According to the function, as the slope approaches zero, the walking speed increases, with the maximum speed of 6 km/h being reached on a slightly downhill slope of approximately -2.9° (Goodchild, 2020, p. 559; Herzog, 2014, p. 232). For a fluid calculation using Tobler's cost function in ArcGIS Pro, Tripcevich (2009) developed an adaptation of the function, aligning with the parameters of the hiking function to represent travel time in hours per meter (h/m). This adaptation, along with his detailed methodological description, served as a template for the calculations used in this study.

3.3.3 Cost Surface 02: Hydrology and slope

To generate the combined Cost Surface 02, a slope raster dataset was merged with hydrological data in QGIS. The slope raster dataset, with each pixel representing the slope inclination angle in degrees, was created using the "Slope" tool from a 10 × 10 m resolution digital terrain model (DTM). For the hydrological features, a watercourse dataset was developed to include major watercourses within the Area of Interest (AOI). This dataset incorporated both actual river paths and potential flood zones, using a 300-year floodplain dataset and applying a 50 m buffer to the Fladnitz, Mank, Melk, and Pielach rivers, expanding their widths to 100 m. A similar 50 m buffer was applied to sections of the Erlauf River to cover gaps not included in the floodplain dataset. Buffering rivers to define geometric regions at a fixed distance is a common GIS technique, and in this instance, QGIS's "Buffer" tool was employed (Conolly & Lake, 2006, p. 209; Herzog & Schröer, 2019, p. 11). The individual watercourse data were rasterized in ArcGIS Pro using the "Mosaic to New Raster" tool to create a single watercourse dataset with a 10 × 10 m resolution. All raster cells representing watercourse areas were assigned the value "5," while cells outside of these areas were given a "NODATA" value. The combined cost surface, incorporating watercourses and slope, was initially classified with values ranging from "1" to "11" based on the German Federal Mapping Guideline KA5 (Ad-hoc-AG Boden, 2005). (Table 4) A further reclassification was performed, where the values "1" to "8" corresponded to the slope gradient classes of KA5. All values above "8" (slopes exceeding 15°/27%) were uniformly assigned the value "50." (Table 5)

Table 4: Combined cost surface "Watercourses and slope gradient" classified according to KA5

KA5: Value	KA5: Designation	Cost surface: Value (KA5)	Slope inclination (° | %)
1	Not inclined	1	< 0,5 | < 1
2	Not to hardly inclined	2	0,5-1| 1-2
3	Very slightly inclined	3	1-2 | 2-3,5
4	Slightly inclined	4	2-3 | 3,5-5
5	Weak to medium-weak inclination	5	3-5 | 5-9
6	Medium inclined	6	5-7 |9-12
7	Medium to strongly inclined	7	7-10 | 12-18
8	Strongly inclined	8	10-15 | 18-27
9	Very strongly inclined	9	15-20 | 27-36
10	steep	10	20-30 | 36-58
11	Steep to very steep	11	> 30 | > 58

Table 5: Reclassified cost raster data set "Watercourses and slope gradient"

<table>
<tr><th>KA5: Value</th><th>KA5: Designation</th><th>cost surface: Value</th><th>Slope inclination (° | %)</th></tr>
<tr><td>1</td><td>Not inclined</td><td>1</td><td>< 0,5 | < 1</td></tr>
<tr><td>≦ 2</td><td>Not to hardly inclined</td><td>2</td><td>0,5-1| 1-2</td></tr>
<tr><td>≦ 3</td><td>Very slightly inclined</td><td>3</td><td>1-2 | 2-3,5</td></tr>
<tr><td>≦ 4</td><td>Slightly inclined</td><td>4</td><td>2-3 | 3,5-5</td></tr>
<tr><td>≦ 5</td><td>Weak to medium-weak inclination</td><td>5</td><td>3-5 | 5-9</td></tr>
<tr><td>≦ 6</td><td>Medium inclined</td><td>6</td><td>5-7 |9-12</td></tr>
<tr><td>≦ 7</td><td>Medium to strongly inclined</td><td>7</td><td>7-10 | 12-18</td></tr>
<tr><td>≦ 8</td><td>Strongly inclined</td><td>8</td><td>10-15 | 18-27</td></tr>
<tr><td>> 8</td><td>Very steeply inclined/steep to very steep</td><td>50</td><td>> 15 | > 27</td></tr>
</table>

3.3.4 Line density

The line density calculation determines the density of linear vector features for each raster cell within a specified circular neighborhood. It sums the lengths of all line segments intersecting the neighborhood and divides this sum by the neighborhood's area. The radius defines the extent of the circular neighborhood, within which the line density is computed.

3.4 Results

- I Walk an Ancient Road: A Straightforward Methodology for Analyzing Intra- and Inter-regional Connectivity Systems along Roman Frontier Zones. Open Supplementary Data: https://doi.org/10.25365/phaidra.536

4 Section 3: Spatial social network analysis (SSNA)

4.1 Data source

- I Walk an Ancient Road: A Straightforward Methodology for Analyzing Intra- and Inter-regional Connectivity Systems along Roman Frontier Zones. Open Supplementary Data: https://doi.org/10.25365/phaidra.536

4.2 Software used

- QGIS 3.10.10-A Coruña with GRASS 7.8.3: https://download.qgis.org/downloads/
- v.net.models 1.0.0 GRASS GIS plugin in QGIS: https://github.com/benducke/Network-reconstruction-tools-for-GRASS-GIS
- Gephi 0.9.2: https://gephi.org/
- Gephi geolayout plugin: https://gephi.org/plugins/#/plugin/geolayout-plugin

4.3 Description

For the SSNA, Gephi was used with edges weighted by real-space Euclidean distances. This method focuses exclusively on rural settlement sites, creating a directed, one-mode network, unlike multiplex networks that analyze various relationships among different entities. Using the Gephi "GeoLayout" plugin, sites were arranged based on their real-space positions for better interpretative understanding. Betweenness centrality, a key measure, was highlighted and later visualized in QGIS. Betweenness centrality quantifies the proportion of shortest paths passing through a node, identifying key points that connect other nodes within the network (Bastian et al., 2009; Collar et al., 2015; Coward, 2013; Freeman, 1977; Gephi Consortium, 2009–ongoing; Groenhuijzen & Verhagen, 2015, 2016, 2017; Horne, 2018; Jacomy, 2021; Mills, 2017; Peeples, 2019).
A combination of the XTENT model and the Minimum Spanning Tree (MST) was further applied to reconstruct an alternative SSN of AOSI-settlements by a hierarchical model-based network reconstruction. The XTENT model, using parameters (k = 1) and (a = 1.5), provided a balance between site size and geographic distance, enabling the generation of a network where larger sites formed broader connections while maintaining realistic cost constraints. Site hierarchy, assigning size values 1 to 3 to the AOSI-sites, was further implemented according to the results of the previously conducted evaluation of the path densities, allowing for a more nuanced understanding of the spatial relationships and social dynamics of the archaeological sites. The MST model minimized total connection costs, optimizing the network for efficiency and resource conservation. This analysis was conducted using the `v.net.models` tool within GRASS GIS and QGIS (Borůvka, 1926; Ducke, 2023; Nešetřil et al., 2001; Renfrew & Level, 1979).

4.4 Results

- I Walk an Ancient Road: A Straightforward Methodology for Analyzing Intra- and Inter-regional Connectivity Systems along Roman Frontier Zones. Open Supplementary Data: https://doi.org/10.25365/phaidra.536

5 Section 4: Visibility analysis (VA)

5.1 Data source

- I Walk an Ancient Road: A Straightforward Methodology for Analyzing Intra- and Inter-regional Connectivity Systems along Roman Frontier Zones. Open Supplementary Data: https://doi.org/10.25365/phaidra.536

5.2 Software used

- QGIS 3.34.x-Prizren: https://www.qgis.org/
- Visibility Analysis 1.4 plugin in QGIS: (Čučković, 2016)

5.3 Description

For the cumulative Visibility Analysis (VA), the QGIS Visibility Analysis plugin was used to generate aggregated binary viewshed raster surfaces from multiple observation points. This method creates cumulative viewsheds, offering a comprehensive overview of visible areas and establishing a visibility network (Brughmans & Brandes, 2017; Čučković, 2016, 2023; Ruggles et al., 1993; Toma, 2018; Wheatley, 1995).

5.4 Results

- I Walk an Ancient Road: A Straightforward Methodology for Analyzing Intra- and Inter-regional Connectivity Systems along Roman Frontier Zones. Open Supplementary Data: https://doi.org/10.25365/phaidra.536

6 Section 5: Ground truthing

6.1 Data source

- I Walk an Ancient Road: A Straightforward Methodology for Analyzing Intra- and Inter-regional Connectivity Systems along Roman Frontier Zones. Open Supplementary Data: https://doi.org/10.25365/phaidra.536
- I Walk an Ancient Road: A Straightforward Methodology for Analyzing Intra- and Inter-regional Connectivity Systems along Roman Frontier Zones. Open Ground Truthing Photoset: https://doi.org/10.25365/phaidra.549
- Land Use/Cover Area Frame Survey" (LUCAS): https://ec.europa.eu/eurostat/web/lucas/database

6.2 Hardware used

- Nikon D300s and Nikon D7500 DSLRs
- Bridge camera: Nkion P900
- Solmeta Geotagger GMAX external GNSS sensor
- DJI Phantom 4 and DJI Inspire 2 UAVs
- Apple iPhone SE 2020 and Samsung A53 smartphones
- Dacia Logan Pick-up coupé utility

6.3 Software used

- QGIS 3.34.x-Prizren: https://www.qgis.org/
- GeoSetter 3.5.3: https://geosetter.de/
- ImportPhotos plugin in QGIS: Kyriakou et al., 2019.
- DART 2.0.22: https://github.com/APTrust/dart

6.4 Description

A total of 1,675 photographs were taken using various devices equipped with internal or external GNSS sensors and cameras, ensuring that all images were geo-tagged for accurate geographical positioning.
Additionally, the "Land Use/Cover Area Frame Survey" (LUCAS) project by Eurostat of the European Commission aims to provide a standardized dataset on current surface cover and use across the European Union (EU), updated at regular intervals (d'Andrimont et al., 2020). This dataset is based on a regular grid of 1,090,863 photo positions distributed across the entire EU. At each position, photos are taken facing north, east, south, and west to document the current state of surface cover and land use, with an additional fifth photo capturing the exact position. This dataset holds significance not only for spatial management and economics but also for archaeology, especially in the context of this thesis. It provides an up-to-date, comprehensive recording of the recent landscape from a first-person perspective, complementing aerial and satellite imagery, and offers insights into the impact of recent construction on archaeological features. Additionally, the LUCAS data enables a large-scale phenomenological survey of the Area of Interest (AOI) without the need for on-site visits, which was particularly valuable during the COVID-19 lockdowns that restricted travel to rural areas. The use of LUCAS data thus also contributed to environmental protection by reducing the need for additional trips. Unlike tools such as Google Street View (https://www.google.com/streetview/) from Alphabet, Inc. or Mapillary (https://www.mapillary.com/) from Meta Platforms, Inc., the LUCAS dataset offers a homogeneous and highly standardized dataset of consistent quality, covering all areas rather than being limited to streets. For this project, Eurostat provided a "LUCAS subsample" for Austria, consisting of 52,927 images from the 2009 and 2015 LUCAS datasets.
The collected photos were curated using the freeware GeoSetter, which checked coordinates and automatically assigned metadata such as height and place names. This data was then imported into GIS using the "ImportPhotos"

plugin in QGIS, which converts the photos into point shapefiles based on their geo-tags, enabling spatial visualization in QGIS.

For archiving the photos taken for ground-truthing, the BagIt format was used (Kunze et al., 2018), conforming to pre-configured BagIt profiles. APTrust's DART tool (Digital Archivist's Resource Tool) was applied for packaging and uploading the images, utilizing the APTrust 2.2 default BagIt profile, with data packed into a single TAR file.

All image data was processed in compliance with the General Data Protection Regulation (GDPR; http://data.europa.eu/eli/reg/2016/679/2016-05-04), to ensure maximum protection of personal data throughout the project.

7 References

Ad-hoc-AG Boden (Ed.). (2005). Monographien von BGR und LBEG. Bodenkundliche Kartieranleitung: KA5 (5th ed.). Schweizerbart.

Bailey, G. (2005). Site Catchment Analysis. In C. Renfrew & P. G. Bahn (Eds.), *Archaeology: The Key Concepts* (pp. 172–176). Taylor and Francis.

Bastian, M., Heymann, S., & Jacomy, M. (2009). Gephi: An Open Source Software for Exploring and Manipulating Networks. *International AAAI Conference on Weblogs and Social Media.* Advance online publication. https://doi.org/10.13140/2.1.1341.1520

Becker, D., Andrés-Herrero, M. de, Willmes, C., Weniger, G.-C., & Bareth, G. (2017). Investigating the Influence of Different DEMs on GIS-Based Cost Distance Modeling for Site Catchment Analysis of Prehistoric Sites in Andalusia. *ISPRS International Journal of Geo-Information*, *6*(2), 1–28. https://doi.org/10.3390/ijgi6020036

Bintliff, J. L. (2000). The Concepts of 'Site' and 'Offsite' Archaeology in Surface Artefact Survey. In M. Pasquinucci & G. Barker (Eds.), *The Archaeology of Mediterranean Landscapes: Vol. 4. Non-destructive Techniques Applied to Landscape Archaeology* (pp. 200–215). Oxbow Books. http://hdl.handle.net/1887/8430

Bintliff, J. L. (2012). Catchments, Settlement Chambers and Demography. In C. Gandini, F. Favory, & L. Nuninger (Eds.), *BAR International Series: Vol. 2370. Settlement Patterns, Production and Trades from the Neolithic to the Middle Ages: Archaedyn, Seven Millennia of Territorial Dynamics. Final Conference, University of Burgundy, Dijon, 23–25 June 2008* (pp. 107–117). Archaeopress.

Bintliff, J. L., & Snodgrass, A. M. (1988). Off-Site Pottery Distributions: A Regional and Interregional Perspective. *Current Anthropology*, *29*, 506–513. http://www.jstor.com/stable/2743472

Borůvka, O. (1926). O jisíém problému minimálním. *Práce Moravské přírodovědecké společnosti*, *3*(3), 36–58. http://hdl.handle.net/10338.dmlcz/500114

Brughmans, T., & Brandes, U. (2017). Visibility Network Patterns and Methods for Studying Visual Relational Phenomena in Archeology. *Frontiers in Digital Humanities*, *4*, Article 17, 1099. https://doi.org/10.3389/fdigh.2017.00017

Casarotto, A. (2017). A Method for Modeling Dispersed Settlements: Visualizing an Early Roman Colonial Landscape as Expected by Conventional Theory. *Archeologia E Calcolatori*, *28*(1), 147–163. https://doi.org/10.19282/ac.28.1.2017.09

Clark, P. J., & Evans, F. C. (1954). Distance to Nearest Neighbor as a Measure of Spatial Relationships in Populations. *Ecology*, *35*(4), 445–453. https://doi.org/10.2307/1931034

Collar, A., Coward, F., Brughmans, T., & Mills, B. J. (2015). Networks in Archaeology: Phenomena, Abstraction, Representation. *Journal of Archaeological Method and Theory*, *22*(1), 1–32. https://doi.org/10.1007/s10816-014-9235-6

Conolly, J., & Lake, M. (2006). *Geographical Information Systems in Archaeology*. Cambridge University Press. https://doi.org/10.1017/CBO9780511807459

Coward, F. (2013). Grounding the Net: Social Networks, Material Culture and Geography in the Epipalaeolithic and Early Neolithic of the Near East (~21,000-6,000 cal bce). In C. Knappett (Ed.), *Network Analysis in Archaeology: New Approaches to Regional Interaction* (pp. 247–280). Oxford University Press. https://doi.org/10.1093/acprof:oso/9780199697090.001.0001

Čučković, Z. (2016). Advanced Viewshed Analysis: A Quantum GIS Plug-in for the Analysis of Visual Landscapes. *The Journal of Open Source Software*, *1*(4), 32. https://doi.org/10.21105/joss.00032

Čučković, Z. (2023). Visibility Networks. In T. Brughmans, B. J. Mills, J. Munson, & M. A. Peeples (Eds.), *The Oxford Handbook of Archaeological Network Research* (pp. 230–247). Oxford University Press. https://doi.org/10.1093/oxfordhb/9780198854265.013.13

d'Andrimont, R., Yordanov, M., Martinez-Sanchez, L., Eiselt, B., Palmieri, A., Dominici, P., Gallego, J., Reuter, H. I., Joebges, C., Lemoine, G., & van der Velde, M. (2020). Harmonised LUCAS in-situ land cover and use database for field surveys from 2006 to 2018 in the European Union. *Scientific Data*, *7*(1), 352. https://doi.org/10.1038/s41597-020-00675-z

Dijkstra, E. W. (1959). A Note on two Problems in Connexion with Graphs. *Numerische Mathematik*, *1*, 269–271. https://doi.org/10.1007/BF01386390

Ducke, B. (2015). Spatial Cluster Detection in Archaeology: Current Theory and Practice. In J. A. Barcelo & I. Bogdanovic (Eds.), *Mathematics and Archaeology* (pp. 352–367).

Ducke, B. (2023). *v.net.models* [Computer software]. https://github.com/benducke/v.net.models

Ester, M., Kriegel, H.-P., Sander, J., & Xu, X. (1996). A Density-based Algorithm for Discovering Clusters in Large Spatial Databases with Noise. In E. Simoudis, J. Han, & U. Fayyad (Eds.), *Proceedings of* 2^{nd} *International Conference on Knowledge Discovery and Data Mining (KDD-96): Portland Oregon. August 2 - 4, 1996* (pp. 226–231).

Forbes, H. (2013). Off-Site Scatters and the Manuring Hypothesis in Greek Survey Archaeology: An Ethnographic Approach. *Hesperia: The Journal of the American School of Classical Studies at Athens*, *82*(4), 551–594. https://doi.org/10.2972/hesperia.82.4.0551

Freeman, L. C. (1977). A Set of Measures of Centrality Based on Betweenness. *Sociometry*, *40*(1), 35. https://doi.org/10.2307/3033543

Gallant, T. W. (1986). "Background Noise" and Site Definition: A Contribution to Survey Methodology. *Journal of Field Archaeology*, *13*, 403–418. https://doi.org/10.2307/530167

Gephi Consortium. (2009–ongoing). *Gephi: The Open Graph Viz Platform*. https://gephi.org/

Gimond, M. (2024). *Intro to GIS and Spatial Analysis*. https://mgimond.github.io/Spatial/index.html

Goodchild, M. F. (2020). Beyond Tobler's Hiking Function. *Geographical Analysis*, *52*(4), 558–569. https://doi.org/10.1111/gean.12253

Groenhuijzen, M. R., & Verhagen, P. (2015). Exploring the Dynamics of Transport in the Dutch *Limes*. *ETopoi. Journal for Ancient Studies*, *4*, 25–47.

Groenhuijzen, M. R., & Verhagen, P. (2016). Testing the Robustness of Local Network Metrics in Research on Archeological Local Transport Networks. *Frontiers in Digital Humanities*, *3*, 509. https://doi.org/10.3389/fdigh.2016.00006

Groenhuijzen, M. R., & Verhagen, P. (2017). Comparing Network Construction Techniques in the Context of Local Transport Networks in the Dutch Part of the Roman *limes*. *Journal of Archaeological Science: Reports*, *15*, 235–251. https://doi.org/10.1016/j.jasrep.2017.07.024

Hagmann, D. (2024). Adopt, Adapt, and Share! FAIR Archeological Data for Studying Roman Rural Landscapes in Northern Noricum. *Journal of Open Humanities Data*, *10*, Article 13. https://doi.org/10.5334/johd.129

Hagmann, D. (in press/2024). A System of Ups and Downs: Roman Rural Landscapes in Northern Noricum. *Journal of Roman Archaeology*.

Herzog, I. (2014). A Review of Case Studies in Archaeological Least-Cost Analysis. *Archeologia E Calcolatori*, *25*, 223–239. http://www.archcalc.cnr.it/indice/PDF25/12_Herzog.pdf

Herzog, I. (2020). Spatial Analysis Based On Cost Functions. In M. Gillings, P. Hacigüzeller, & G. R. Lock (Eds.), *Archaeological Spatial Analysis: A Methodological Guide* (pp. 333–358). Routledge, Taylor & Francis Group. https://doi.org/10.4324/9781351243858-18

Herzog, I., & Schröer, S. (2019). Reconstruction of Roman Roads and Boundaries in Southern Germany. In *Proceedings of the 22nd International Conference on Cultural Heritage and New Technologies 2017: CHNT 22, 2017 (Vienna 2019)* (pp. 1–19). Selbstverlag. https://www.chnt.at/wp-content/uploads/eBook_CHNT22_Herzog-Schroeer.pdf

Horne, R. M. (2018, November 11). *What Do You Do with 36,409 Places and 6,506 Connections? Some Cartographic Representations of Pleiades Data*. https://rmhorne.org/2018/11/11/what-do-you-do-with-36409-places-and-6506-connections-some-cartographic-representations-of-pleiades-data/

Jacomy, A. (2021, May 30). *GeoLayout: The Gephi plugin to map geocoded graph data*. GitHub. https://github.com/jacomyal/GeoLayout

Kunze, J., Littman, J., Madden, E., Scancella, J., & Adams, C. (2018). *The BagIt File Packaging Format (V1.0).* https://doi.org/10.17487/RFC8493

Kyriakou, M., Christou, G., & Kolios, P. (2019). *Importphotos: A QGIS Plugin to Visualise Geotagged Photos*.

Legg, R. J. (2008). Sites: Catchment Analysis. In D. M. Pearsall (Ed.), *Encyclopedia of Archaeology* (pp. 2002–2004). Elsevier. https://doi.org/10.1016/B978-012373962-9.00283-1

McCoy, M. D. (2020). The Site Problem: A Critical Review of the Site Concept in Archaeology in the Digital Age. *Journal of Field Archaeology*, *45*(sup1), S18-S26. https://doi.org/10.1080/00934690.2020.1713283

Mehrer, M., & Westcott, K. L. (Eds.). (2006). *Gis and Archaeological Site Location Modeling*. Tayler & Francis. https://doi.org/10.1201/9780203563359

Mills, B. J. (2017). Social Network Analysis in Archaeology. *Annual Review of Anthropology*, *46*(1), 379–397. https://doi.org/10.1146/annurev-anthro-102116-041423

Nešetřil, J., Milková, E., & Nešetřilová, H. (2001). Otakar Borůvka on minimum spanning tree problem Translation of both the 1926 papers, comments, history. *Discrete Mathematics*, *233*(1-3), 3–36. https://doi.org/10.1016/S0012-365X(00)00224-7

Orton, C. (2004). Point Pattern Analysis Revisited. *Archeologia E Calcolatori*, *15*, 299–315. http://www.archcalc.cnr.it/journal/id.php?id=oai:www.archcalc.cnr.it/journal/A_C_oai_Archive.xml:373

Peeples, M. A. (2019). Finding a Place for Networks in Archaeology. *Journal of Archaeological Research*, *27*(4), 451–499. https://doi.org/10.1007/s10814-019-09127-8

Pelgrom, J. (2018). The Roman Rural Exceptionality Thesis Revisited. *Mélanges De L'école Française De Rome. Antiquité.* Advance online publication. https://doi.org/10.4000/mefra.4770

Pinder, D., Shimada, I., & Gregory, D. (1979). The Nearest-Neighbor Statistic:. *American Antiquity*, *44*(3), 430–445. https://doi.org/10.2307/279543

Renfrew, C., & Level, E. V. (1979). Exploring Dominance: Predicting Polities from Centers. In C. Renfrew & K. L. Cooke (Eds.), *Transformations* (pp. 145–167). Elsevier. https://doi.org/10.1016/B978-0-12-586050-5.50016-6

Rivers, R., Knappett, C., & Evans, T. (2013). What Makes a Site Important? Centrality, Gateways, and Gravity. In C. Knappett (Ed.), *Network Analysis in Archaeology: New Approaches to Regional Interaction* (pp. 125–150). Oxford University Press. https://doi.org/10.1093/acprof:oso/9780199697090.003.0006

Ruggles, C. L. N., Medyckyj-Scott, D. J., & Gruffydd, A. (1993). Multiple Viewshed Analysis Using GIS and Its Archaeological Applicatio: A Case Study in Northern Mull. In J. Andresen, T. Madsen, & I. Scollar (Eds.), *Computing the Past: Computer Applications and Quantitative Methods in Archaeology. CAA92* (125-132). Aarhus University Press.

Schubert, E., Sander, J., Ester, M., Kriegel, H. P., & Xu, X. (2017). DBSCAN Revisited, Revisited. *ACM Transactions on Database Systems*, *42*(3), 1–21. https://doi.org/10.1145/3068335

Schulzki, H.-J. (2006a). Leuga. In H. Cancik, H. Schneider, & M. Landfester (Eds.), *Der Neue Pauly Online: Antike. Rezeptions- und Wissenschaftsgeschichte.* https://doi.org/10.1163/1574-9347_bnp_e702490

Schulzki, H.-J. (2006b). Pes. In H. Cancik, H. Schneider, & M. Landfester (Eds.), *Der Neue Pauly Online: Antike. Rezeptions- und Wissenschaftsgeschichte.* https://doi.org/10.1163/1574-9347_dnp_e916020

Surface-Evans, S. L., & White, D. A. (2012). An Introduction to the Least Cost Analysis of Social Landscapes. In D. A. White & S. L. Surface-Evans (Eds.), *Least Cost Analysis of Social Landscapes: Archaeological Case Studies* (pp. 1–7). University of Utah Press.

Tobler, W. (1993). Three Presentations on Geographical Analysis and Modeling: Non-Isotropic Geographic Modeling. Speculations on the Geometry of Geography. Global Spatial Analysis. *National Center for Geographic Information and Analysis – Technical Report*, *93*(1), 1–25. https://escholarship.org/content/qt05r820mz/qt05r820mz.pdf

Toma, L. (2018). Viewshed Analysis. In S. L. López Varela (Ed.), *The Encyclopedia of Archaeological Sciences* (pp. 1–6). Wiley. https://doi.org/10.1002/9781119188230.saseas0595

Tripcevich, N. (2009). Tobler's walking model using Optimal Path as Line or Pathdistance in ArcGIS. *Unpublished Papers and Presentations*, *30c414w4*. https://escholarship.org/uc/item/30c414w4

Verhagen, P., Vossen, I., Groenhuijzen, M. R., & Joyce, J. (2016). Now You See Them, Now You Don't: Defining and Using a Flexible Chronology of Sites for Spatial Analysis of Roman Settlement in the Dutch River Area. *Journal of Archaeological Science: Reports*, *10*, 309–321. https://doi.org/10.1016/j.jasrep.2016.10.006

Vita-Finzi, C., Higgs, E. S., Sturdy, D., Harriss, J., Legge, A. J., & Tippett, H. (1970). Prehistoric Economy in the Mount Carmel Area of Palestine: Site Catchment Analysis. *Proceedings of the Prehistoric Society*, *36*, 1–37. https://doi.org/10.1017/S0079497X00013074

Wheatley, D. (1995). Cumulative Viewshed Analysis: A GIS-based method for investigating intervisibility, and its archaeological application. In G. R. Lock & Z. Stančič (Eds.), *Archaeology and Geographical Information Systems: A European Perspective* (pp. 171–185). Taylor and Francis.

Wheatley, D., & Gillings, M. (2002). *Spatial Technology and Archaeology: The Archaeological Applications of GIS*. Taylor and Francis. https://doi.org/10.1201/b12806

Wilkinson, T. J. (1989). Extensive Sherd Scatters and Land-Use Intensity: Some Recent Results. *Journal of Field Archaeology*, *16*(1), 31. https://doi.org/10.2307/529879

Witcher, R. E. (2012). "That From A Long Way Off Look Like Farms": The Classification of Roman Rural Sites. In P. A. J. Attema & G. Schörner (Eds.), *Journal of Roman Archaeology. Supplementary Series: Vol. 88. Comparative Issues in the Archaeology of the Roman Rural Landscape: Site Classification Between Survey, Excavation and Historical Categories* (pp. 11–30). Journal of Roman Archaeology.